JMEPEG (2015) 24:2546–2555
DOI: 10.1007/s11665-015-1519-9

1059-9495/$19.00

Weld Growth Mechanisms and Failure Behavior of Three-Sheet Resistance Spot Welds Made of 5052 Aluminum Alloy

Yang Li, Fuyu Yan, Zhen Luo, Y.J. Chao, Sansan Ao, and Xuetuan Cui

(*Submitted May 30, 2014; in revised form April 1, 2015; published online April 18, 2015*)

This paper investigates the weld nugget formation in three-sheet aluminum alloy resistance spot welding. The nugget formation process in three equal thickness sheets and three unequal thickness sheets of 5052 aluminum alloy were studied. The results showed that the nugget was initially formed at the workpiece/workpiece interfaces (i.e., both upper interface and lower interface). The two small nuggets then grew along the radial direction and axial direction (welding direction) as the welding time increased. Eventually, the two nuggets fused into one large nugget. During the welding process, the Peltier effect between the Cu-Al caused the shift of the nugget in the welding direction. In addition, the mechanical strength and fracture mode of the weld nuggets at the upper and lower interfaces were also studied using tensile shear specimen configuration. Three failure modes were identified, namely interfacial, mixed, and pullout. The critical welding time and critical nugget diameter corresponding to the transitions of these modes were investigated. Finally, an empirical failure load formula for three-sheet weld similar to two-sheet spot weld was developed.

Keywords aluminum alloy, failure behavior, Peltier effect, resistance spot welding, three sheets, weld growth mechanisms

1. Introduction

Resistance spot welding (RSW) is a very effective method to join two or more thin metal sheets using heat produced by electric current flowing through workpieces and electrodes. The automotive industry makes extensive use of the RSW with typically 4000-6000 spot welds in a motor car. Nowadays, most RSW studies are limited to two-sheet assemblies and less attention is paid to spot welding of multiple sheets (Ref 1-4). However, with the demand of lightweight vehicle structures, RSW of multiple stacks of similar or dissimilar workpieces is increasingly applied in some complex structures such as front longitudinal rails, A-, B-, and C-pillars, and the bulkhead to inner wing (Ref 5). Compared to two-sheet spot welding, joining three sheets is significantly more complicated because of the extra interface introduced and the lack of past experience in this configuration. The use of different material combinations and/or non-uniform sheet thickness in the three layers complicates the process even further.

Yang Li, Fuyu Yan, Zhen Luo, Sansan Ao, and **Xuetuan Cui**, 25-C-810, School of Materials Science and Engineering and Tianjin Key Laboratory of Advanced Joining Technology, Tianjin University, No. 92 Weijin Road, Tianjin 300072, China; and **Y.J. Chao**, 25-C-703, School of Materials Science and Engineering and Tianjin Key Laboratory of Advanced Joining Technology, Tianjin University, No. 92 Weijin Road, Tianjin 300072, China; and Department of Mechanical Engineering, University of South Carolina, Columbia, SC. Contact e-mail: lz_tju@163.com.

One of the most important issues in RSW of three-sheet joints is insufficient growth of the weld nugget, which may cause problems in places needing larger weld nuggets at sheet/sheet interface to provide sufficient strength.

Some researchers have investigated the nugget growth and mechanical behavior of three-sheet RSW. Harlin et al. (Ref 6) investigated the weld growth mechanisms during RSW of two and three steel sheets. They suggested that the position of initial heat generation is independent of material thickness and stack configuration. They also found that increasing the electrode force leads to a shift in the initial position of weld nugget formation from the sheet/sheet interface to the center of the middle sheet (Ref 7). Pouranvari and Marashi (Ref 8) studied the effect of sheet thickness on the pattern of weld nugget development during RSW of three steel sheets of equal thickness. They found that for a critical sheet thickness of 1.5 mm, the size of the fusion zone at the sheet/sheet interface is nearly equal to that of the fusion zone at the geometrical center of the joint.

Many other studies using finite element (FE) simulation investigated the nugget formation process of three-sheet steel spot welds. Lei et al. (Ref 9) built a two-dimensional FE model considering the thermal-electrical coupling for RSW process of mild steel. Ma and Murakawa (Ref 10) developed an FE program considering the coupling of electrical, thermal, and mechanical fields to study the nugget formation in RSW of high-strength steels.

Although many studies have performed on weld growth process of three-sheet spot welds, these researches all focused on the mild steel and high-strength steels. At present, very little work in open literature studied the RSW of multiple aluminum alloy sheets. Aluminum alloy is used more frequently in the automotive industry for its lightweight, good formability, machinability, and high corrosion resistance (Ref 11). At the same time, aluminum alloy has higher thermal and electrical conductivity, varied metallurgical properties, and oxide layers that complicate the nugget formation process when compared with that of steel sheets.

This paper investigates the weld nugget growth in three-sheet spot welds made of 5052 aluminum alloy. The nugget formation process of both three equal thickness sheets and three unequal thickness sheets were studied. We focused on the initial position of heat generation, nugget formation, and nugget growth during the welding process in these sheet configurations. Tensile shear tests were performed on the upper interface and lower interface weld nuggets in the three-sheet combination to investigate the failure mechanisms and strength of the welds.

2. Experimental Procedures

The material used in the experiments was AA5052 with its chemical composition and mechanical properties listed in Tables 1 and 2.

Welding was performed on a 220 kW direct current (DC) inverter RSW machine. Truncated cone electrodes with a 6-mm-diameter tip end made of copper alloy of RWMA class II chrome were used as the electrodes for the welding. To study the weld formation at different welding times, the welding time was chosen to start from a low value and gradually increased to a value when expulsion started, while other parameters were held constant. The welding parameters are shown in Table 3. Two three-sheet configurations were used in the experiments. From the upper electrode tip to the lower one, the two three-sheet configurations were 2.0/2.0/2.0 and 1.0/1.5/2.0 mm, respectively.

After welding, microscope and stereomicroscope were used to observe the metallographic and nugget morphology. Figure 1 is the nugget diameter and height measurement parameters, where s_1 and s_2 are the nugget diameters at the upper and lower interfaces, respectively; h_1 and h_2 are the nugget heights at the upper and lower interfaces, respectively; H_1, H_2, and H_3 are the thicknesses of the individual sheet.

3. Weld Formation in Three Equal and Unequal Thickness Stacks

3.1 Three Equal Thickness Sheets (2.0/2.0/2.0 mm)

The stereomicroscope results of the nuggets cross section with different welding times are shown in Fig. 2. It can be seen that when the welding time was 40 ms (Fig. 2a), two nuggets formed at the two interfaces simultaneously. With the increase in welding time, the two small nuggets at the upper and lower interfaces grew slowly along both the radial and the axial (height) directions of the workpieces, and fused into one nugget, which looks like the letter "I" (Fig. 2c). As the welding time continued to increase, the "I"-shaped nugget grew in both radial and axial directions. Eventually, at the welding time of 350 ms, the nugget grew into an elliptical shape with the maximum nugget diameter located at the center of the middle sheet.

Figure 3 shows the numerical values of the nugget sizes at the two interfaces with welding time during RSW. Note that the nugget diameter at the upper interface was always larger than that at the lower interface. It can be explained by the Peltier effect.

Peltier effect is a phenomenon when a direct current goes through a joint of two conductors with different conductivities; heat will be liberated or absorbed at the junction depending on the current direction (Ref 12). During RSW of aluminum alloy, as the electrode material is copper (Cu), the Cu-Al junction has a high contact potential difference, which makes the Peltier effect more obvious (Ref 13). When the upper electrode tip is positive, heat is generated at the upper electrode/workpiece (i.e., Cu-Al) interface, while heat is absorbed at the lower interface (i.e., Al-Cu) according to the Peltier effect (Ref 13). This causes the temperature in the upper interface higher than the lower interface resulting in a slightly larger nugget at the upper interface. The difference in nugget size is much more pronounced in the height (axial) direction, as shown in Fig. 4.

In Fig. 3, the minimum acceptable nugget diameter, $4\sqrt{t}$, where t is the sheet thickness, is also plotted, which according to the AWS D8.9M:2012 standard (Ref 14) is the minimum nugget diameter without metal expulsion and to ensure its strength. In this case, $4\sqrt{t} = 5.66$ mm for $t = 2$ mm occurred at welding time slightly less than 150 ms. After 150 ms, the nugget formation was stabilized.

3.2 Three Unequal Thickness Sheets (1.0/1.5/2.0 mm)

The stereomicroscope results of the nuggets cross section with different welding times for the RSW of three unequal thickness sheets (1.0/1.5/2.0 mm) are shown in Fig. 5.

Similar to the case of three equal thickness sheets, when the welding time was short, two small nuggets were observed at the upper and lower interfaces, and the nugget diameter in the upper or 1.0/1.5 interface was larger than that at the lower or 1.5/2.0 interface (see Fig. 5a). This is another evidence of the Peltier effect which results in more heat generation at the Cu-Al side than at the Al-Cu side. Again, two small nuggets grew slowly along both the radial and the axial directions of the workpieces and then fused into an "I"-shaped nugget at 40-ms welding time.

Once the nugget was formed, the nugget growth in the 1.5/2.0 interface was faster than in the 1.0/1.5 mm interface, and the center of the nugget shifted slowly toward the 2.0-mm sheet. Note that once the nugget was formed, the metal was

Table 2 Mechanical properties of 5052 aluminum alloy

Sample temper	Yield strength, MPa	Tensile strength, MPa	Elongation at fracture, %
0	78.9	201.7	15

Table 1 Chemical composition of 5052 aluminum alloy (wt.%)

Al	Mg	Cr	Si	Fe	Cu	Mn	Zn	Others
95.70	2.2-2.8	0.15-0.35	≤ 0.25	≤ 0.40	≤ 0.10	≤ 0.10	≤ 0.10	≤ 0.15

melted and the contact resistance disappeared. The heat generation is then purely from the bulk resistance according to Joule's law. Since the thick plate has a higher resistance than the thin plate, more heat was generated near the bottom part, i.e., 1.5/2.0 sheets. Moreover, the 1.5/2.0 interface is far away from the electrode tips than the 1.0/1.5 interface, so the 1.5/2.0 mm interface lose lesser heat than the 1.0/1.5 interface. This effect overweighted the Peltier effect and therefore, the nugget shifted slowly toward the 2.0-mm sheet.

Figure 6 shows the growth of weld nugget as a function of welding time for the unequal thickness sheets 1.0/1.5/2.0 mm. The nugget grew faster along the 1.5/2.0 interface in both directions after 80 ms.

In Fig. 7, one can see that the nugget height at 1.5/2.0 interface kept increasing, while that at the 1.0/1.5 interface remained almost unchanged during the nugget growth process. Although the Peltier effect generated more heat at the 1.0/1.5 side than at the 1.5/2.0 side initially, the 1.0/1.5 side was closer to the water-cooled electrode tip, which transferred heat more quickly and limited the growth of nugget at the 1.0/1.5 interface.

Table 3 Welding parameters used for three sheets with different sheet thicknesses

	Thickness combinations H_1/ H_2/ H_3 (mm)	
Welding parameters	**2.0/2.0/2.0**	**1.0/1.5/2.0**
Electrode force (kN)	3.6	3
Welding current (kA)	18	16
Welding time (ms)	40, 50-400 (increments of 50)	30, 40-300 (increments of 20)
Electrode tip diameter (mm)	6	6

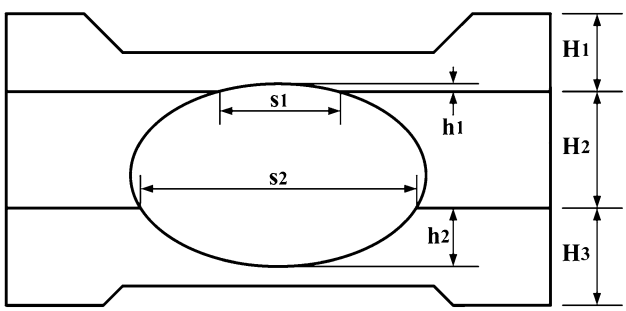

Fig. 1 Nugget size measurement for three-sheet RSW

3.3 Microstructure of Weld Nugget

Since the microstructures in the two three-sheet configurations are similar, only the microstructure of weld nugget in the 2.0/2.0/2.0 mm configuration is presented here. Figure 8 shows the microstructure of weld nugget at welding time of 50 and 200 ms. When the welding time was short, as mentioned in section 3.1, two nuggets formed at the two interfaces simultaneously. A very thin columnar crystal zone (CCZ) emerged at the edge of weld nugget, as shown in Fig. 8(b). Between the two nuggets, the base metal was partially melted, and therefore a partially melted zone (PMZ) is located between the two nuggets (see Fig. 8c). The interior of the weld nugget was equiaxed crystal zone (ECZ). The ECZ is composed of

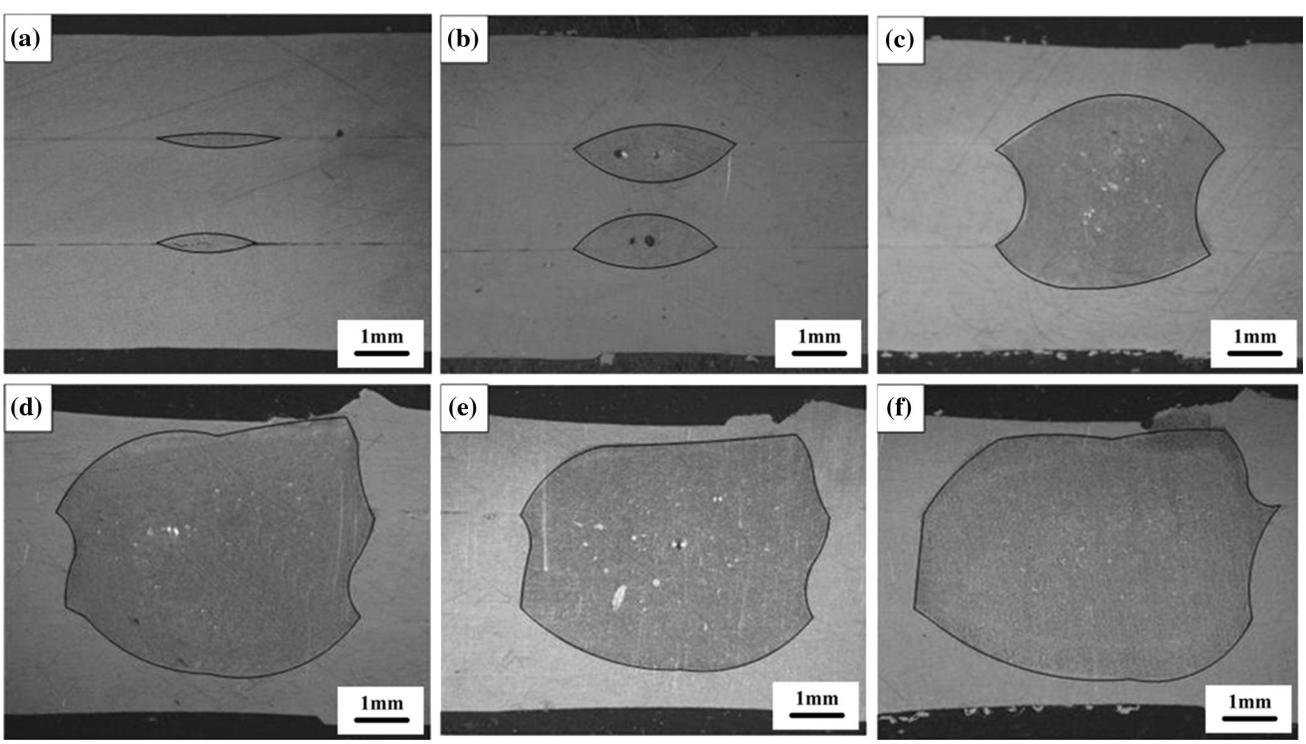

Fig. 2 Growth of weld nugget for equal thickness three-sheet aluminum alloy at welding time: (a) 40 ms, (b) 50 ms, (c) 100 ms, (d) 150 ms, (e) 200 ms, and (f) 350 ms

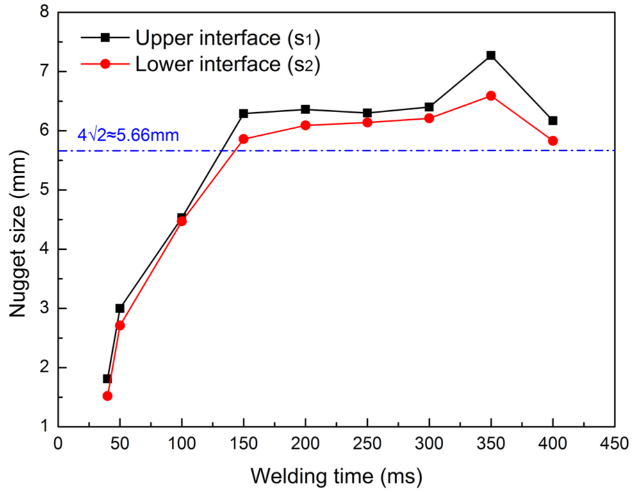

Fig. 3 Growth of weld nugget as function of time at the two interfaces of 2.0/2.0/2.0 mm 5052 aluminum alloy

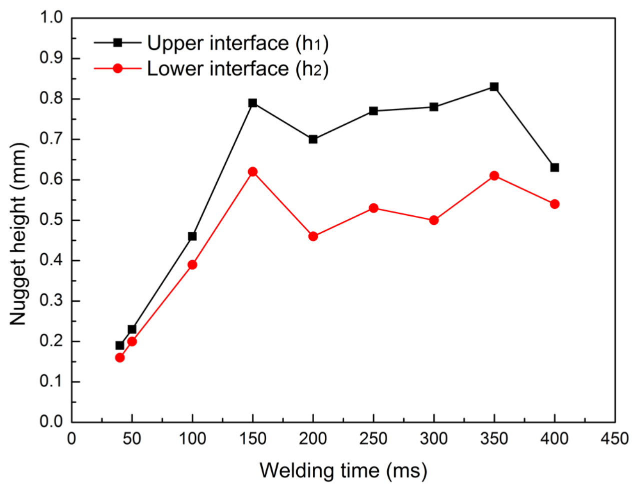

Fig. 4 Growth of weld nugget heights as function of time at the two interfaces of 2.0/2.0/2.0 mm 5052 aluminum alloy

equiaxed grain α(Al) and precipitated phase β(Al_3Mg_2), as shown in Fig. 8(d). Compared with the welding time of 50 ms, when the welding time reached 200 ms, the principal difference of microstructures between the two weld nuggets is the cellular dendrite crystal and columnar dendrite crystal. During the solidification process, the weld microstructure can be divided into five types of crystal morphology according to temperature gradient and constituent supercooling: planar crystal, cellular crystal, cellular dendrite crystal, dendrite crystal, and equiaxed crystal (Ref 15). The peak temperature in weld nugget made at welding time of 50 ms is lower than the weld nugget made at welding time of 200 ms, which lowers the temperature gradient in the weld nugget and therefore promotes the formation of equiaxed crystal and limits the formation of columnar crystal.

4. Tensile Shear Test

While there are many studies on two-sheet resistance spot welds, the studies on mechanical behavior of spot welds made of three sheets is very limited. Tavasolizadeh et al. (Ref 16) investigated the mechanical performance of three-sheet resistance spot welds made of low-carbon steel. The weld nugget growth with welding time of equal thickness sheets was studied and the minimum welding time which borders the failure mode from interface to pullout fracture was determined.

In this paper, the mechanical behavior of the three-sheet spot welds made of 5052 aluminum alloy is studied using tensile shear test. Tests were performed on two configurations for welds made with welding parameters shown in Table 3. The dimension of specimen is 100×25 mm^2 according to GB 2651-88 (Ref 17), as shown in Fig. 9. The tensile shear test specimens were designed to investigate the mechanical behavior at the upper and lower interfaces of the three-sheet spot welds.

Similar to the steel spot welds, three types of failure mode were observed from welds made of different welding times or nugget sizes. The three types, interfacial failure (IF), mixed or partial pullout failure (MF), and pullout failure (PF), are depicted in Fig. 10.

4.1 Peak Load of Equal Thickness Three-Sheet Welds (2.0/2.0/2.0 mm)

The effect of welding time on the peak load of equal thickness three-sheet 5052 aluminum alloy spot welds is shown in Fig. 11. It is shown that as the welding time increased, the peak load increased as well due to larger weld nuggets shown in Fig. 3. In addition, there is a transition in the failure mode from IF to MF, and then to PF as the welding time increased. In engineering applications, IF is often undesirable as it means low-energy absorption capability. The driving force for the IF, MF, and PF modes is the shear stress at the sheet/sheet interface and the tensile stress at the weld nugget borders, respectively (Ref 18, 19). A minimum welding time of 150 ms should be used to avoid IF mode in 2.0/2.0/2.0 mm 5052 aluminum alloy RSW as can be seen from the data in Fig. 11. To obtain a better quality nugget, welding time of at least 350 ms needs to be used to achieve PF.

Weld fusion (weld nugget) size is the most important factor affecting spot weld mechanical strength (Ref 20). As the welding time increased, while other welding parameters were kept unchanged as shown in Table 3, the weld nugget increased in diameter or size. Figure 12 shows the effect of button size on the peak load at both upper and lower interfaces. Here the "button size" is the nugget diameter measured after failure of the welded joint, while the term "nugget size" in previous discussions were measured from the micrograph of the cut and polished cross section of the weld. Since the weld nugget includes a heat-affected zone, the nugget diameter (in Fig. 3) was always slightly bigger than the button size.

Three distinguished failure modes were observed for welds of different button sizes. For the upper interface, the critical button diameter from IF to MF was 5.75 mm, and from MF to PF was 6.60 mm. For the lower interface, the critical button diameter from IF to MF was 5.35 mm, and from MF to PF was 6.40 mm, which is smaller than the upper interface. The small difference is attributed to the Peltier effect which made the nuggets size slightly different at the upper and lower interfaces.

Note that the minimum nugget or button size is $4\sqrt{t} = 5.66$ mm for $t = 2$ mm as specified in Ref 13 for automotive applications. As shown in Fig. 12, this value coincides approximately with our data in transition from IF to

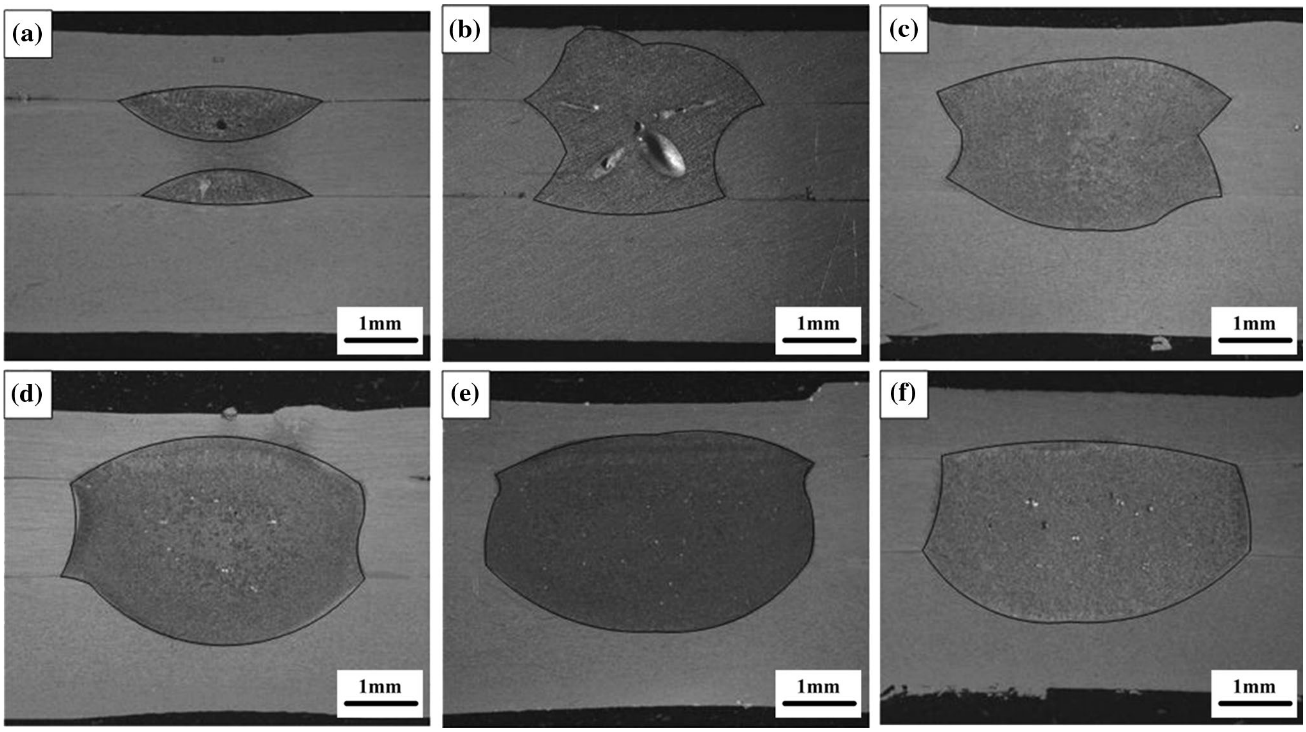

Fig. 5 Growth of weld nugget for unequal thickness three sheets of 1.0/1.5/2.0 mm 5052 aluminum alloy at welding time: (a) 30 ms, (b) 40 ms, (c) 60 ms, (d) 100 ms, (e) 200 ms, (f) 300 ms

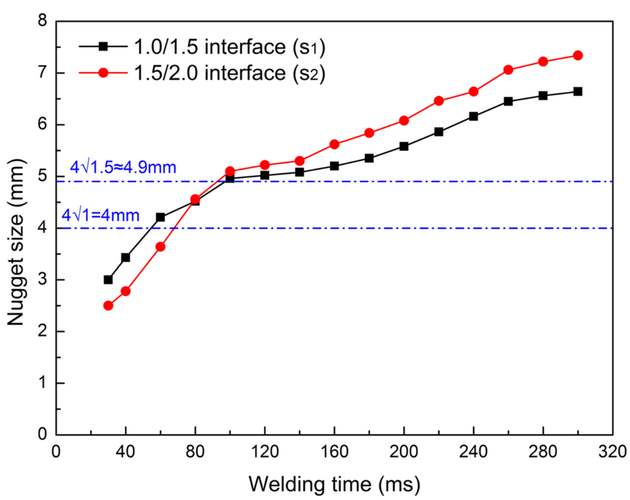

Fig. 6 Growth of weld nugget size as a function of welding time at the two interfaces of 1.0/1.5/2.0 mm 5052 aluminum alloy

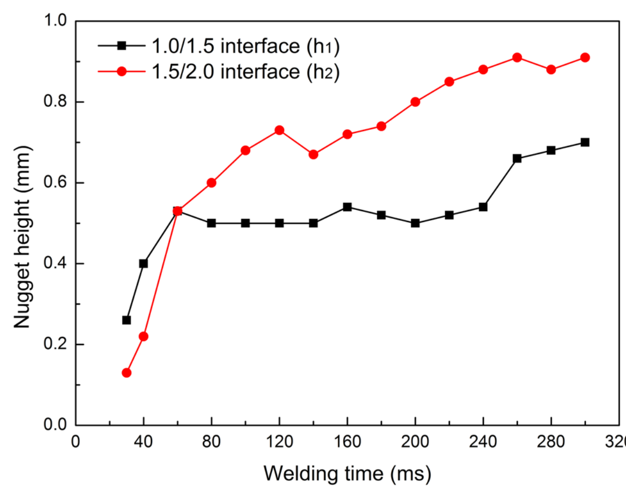

Fig. 7 Growth of weld nugget height as function of welding time at the two interfaces of 1.0/1.5/2.0 mm 5052 aluminum alloy

MF. The optimum weld diameter suggested by Rivett (Ref 21) is $5\sqrt{t} = 7.1$ mm for $t = 2$ mm, which falls in the PF region and therefore guarantees PF mode of failure if optimum weld diameter is applied as a guideline in welding.

4.2 Peak load of Unequal Thickness Three-Sheet Welds (1.0/1.5/2.0 mm)

The effect of welding time on the peak load of unequal thickness three-sheet welds is shown in Fig. 13. When the welding time was short, such as 30 or 40 ms, the peak load of the upper 1.0/1.5 interface was higher than that of the lower 1.5/2.0 interface as the nugget was slightly larger. As the welding time increased to 80 ms, the 1.0/1.5 interface experienced MF mode and at 100 ms emerged in PF mode. For the lower 1.5/2.0 interface, the transition welding time from IF mode to MF was 100 ms and from MF mode to PF mode was 260 ms. In engineering practice, if the upper (lower) interface is subjected to higher load or more critical compared to the lower (upper) interface, the welding time of at least 100 ms (260 ms) should be used to ensure a PF mode. Unlike the case of equal thickness, the large difference between the transition welding times is due to the large difference in sheet thickness at the two interfaces.

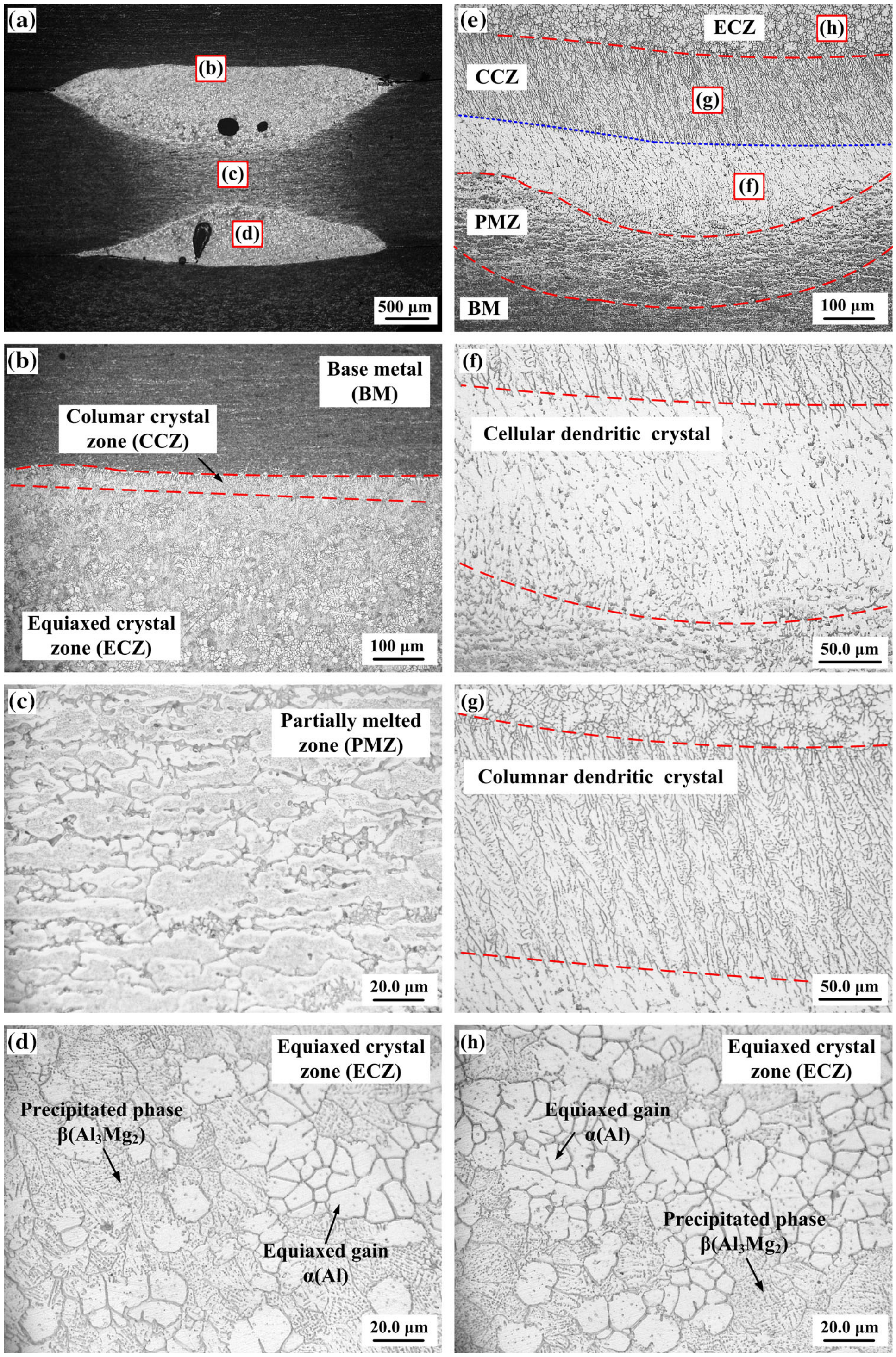

Fig. 8 Microstructure of three-sheet aluminum alloy resistance spot weld: (a)-(d) welding time of 50 ms, (e)-(h) welding time of 200 ms

Figure 14 shows the plot of the peak loads versus button size. The peak load increased with the increase of the button size. All the three failure modes, the IF, MF, and then PF are observed as the button size of the welds increases. For the 1.0/1.5 interface, the transition button size for transition from IF to MF was 4.45 mm and from MF to PF was 4.90 mm. For the 1.5/2.0 interface, the button size for transition from IF to MF was 5.00 mm, and 7.00 mm from MF to PF. Therefore, to ensure PF, the button size should be larger than 4.90 mm for 1.0/1.5 interface and 7.00 mm for 1.5/2.0 interface. Again the large difference here is due to the difference in sheet thickness at the two interfaces.

To correlate the failure mode of spot welds composed of unequal thickness sheets to industry standards of nugget size, such as the minimum nugget size $4\sqrt{t}$ (Ref 14) and the optimal nugget size $5\sqrt{t}$ (Ref 21), one has to revise the thickness t used in the formula as the formula was derived for spot welds of equal thickness sheets. As the failure load of a spot weld made of two unequal thickness, e.g., A/B with A > B, will be higher (lower) than that of B/B (A/A), it is proposed to use the average of the two unequal thicknesses at an interface to interpret the failure mode of the nugget at this particular interface. Using the average, e.g., $t = 1.25$ mm for the upper interface and 1.75 mm for the lower interface of the 1.0/1.5/2.0 mm combination, the minimum button sizes, $4\sqrt{t} = 4.47$ mm for the upper interface and 5.29 mm for the lower interface, appear to coincide with the transition from IF to MF as shown in Fig. 14, i.e., 4.45 and 5.0 mm for the upper interface and lower interface, respectively. Furthermore, the optimum weld diameters, $5\sqrt{t} = 5.59$ and 6.61 mm for the upper interface and lower interface, respectively, appear to exceed the nugget size at the transition from MF to PF, and therefore guarantee a PF failure mode as can been seen from the data in Fig. 14.

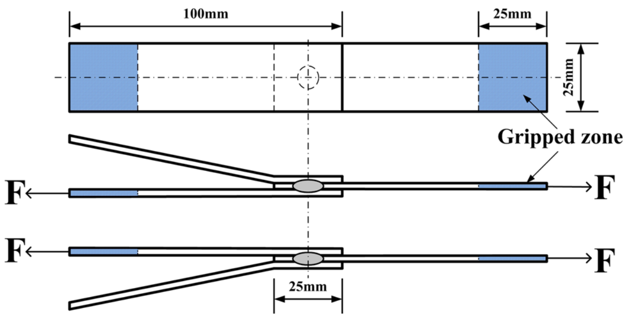

Fig. 9 The sample size and joint design for tensile shear test

4.3 Failure Load Formula

Several models for predicting failure loads of resistance spot welds made of steels were developed in the past (Ref 20, 21, 23). They were typically empirical and based on large amount of test data. For two-sheet spot welds made of steels, a relatively simple formula relating the peak load to sheet thickness, nugget size and ultimate tensile strength of the base metal can be written as (Ref 22).

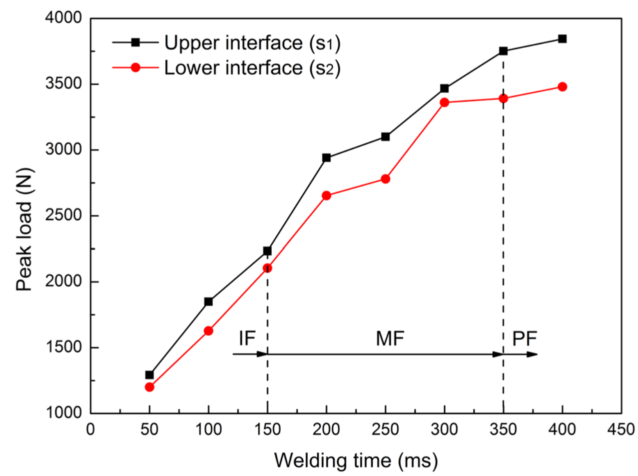

Fig. 11 Effect of welding time on the peak load of 2.0/2.0/2.0 mm three-sheet 5052 aluminum alloy

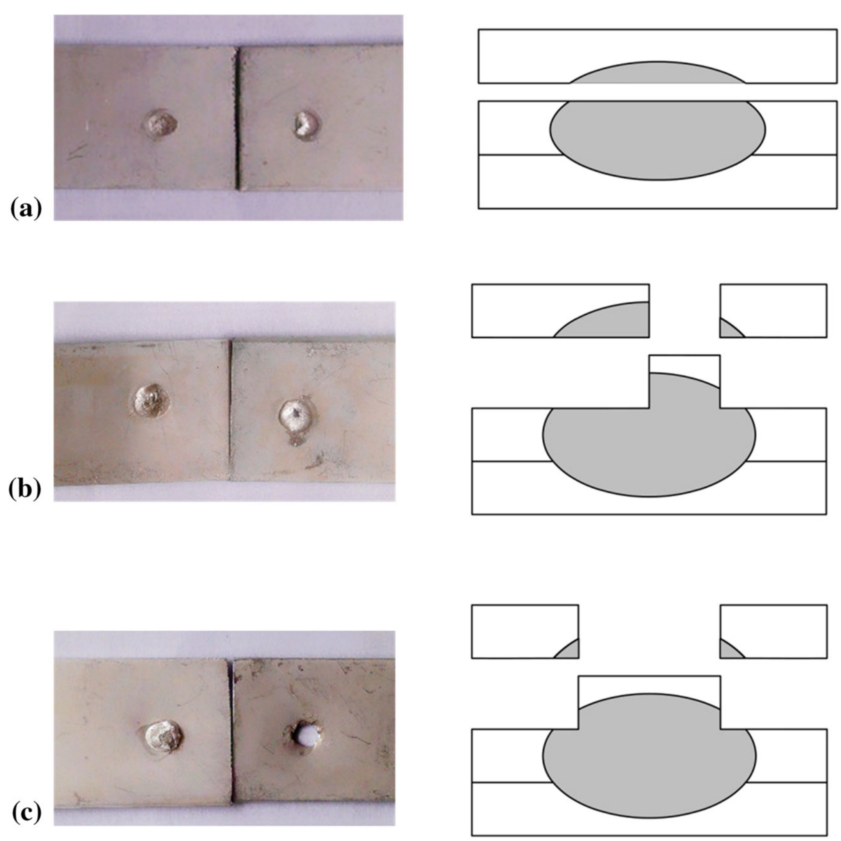

Fig. 10 Three typical fracture modes of three-sheet 5052 aluminum alloy spot welds: (a) interfacial fracture, (b) mixed fracture, and (c) pullout fracture

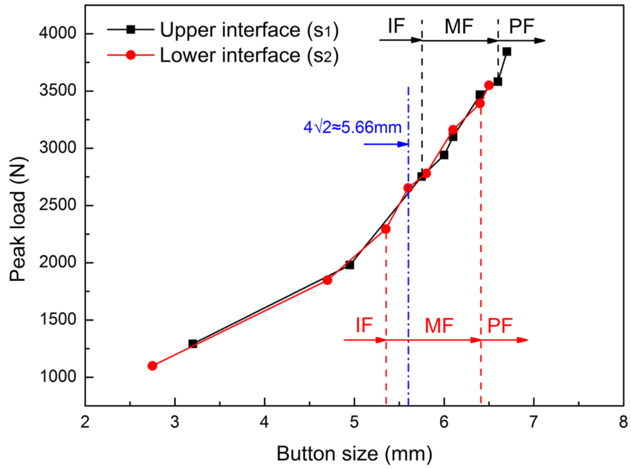

Fig. 12 Effect of button size on the peak load of 2.0/2.0/2.0 mm three-sheet 5052 aluminum alloy

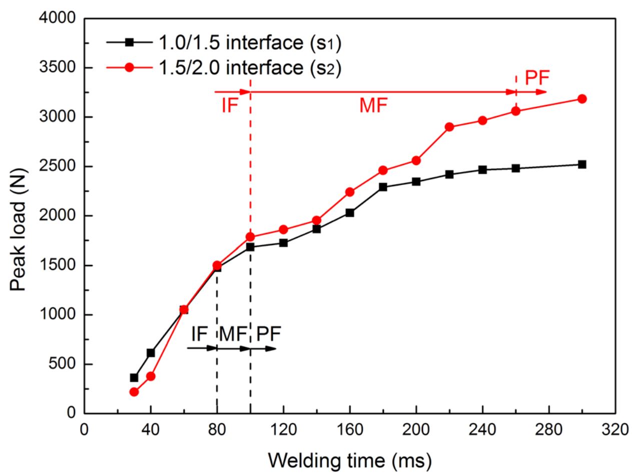

Fig. 13 Effect of welding time on the peak load of 1.0/1.5/2.0 mm three-sheet 5052 aluminum alloy

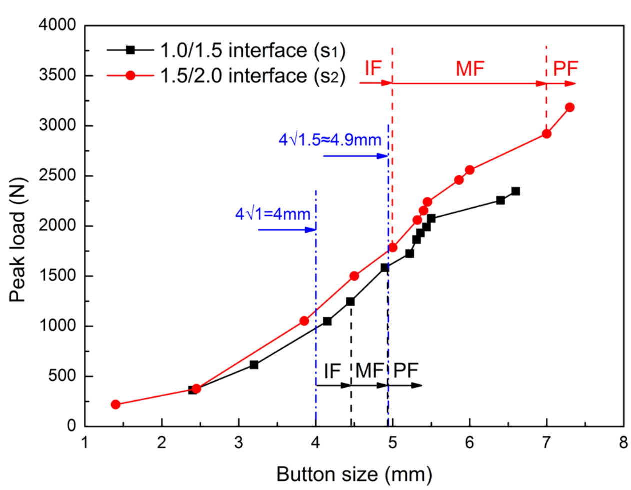

Fig. 14 Effect of button size on the peak load of 1.0/1.5/2.0 mm three-sheet 5052 aluminum alloy

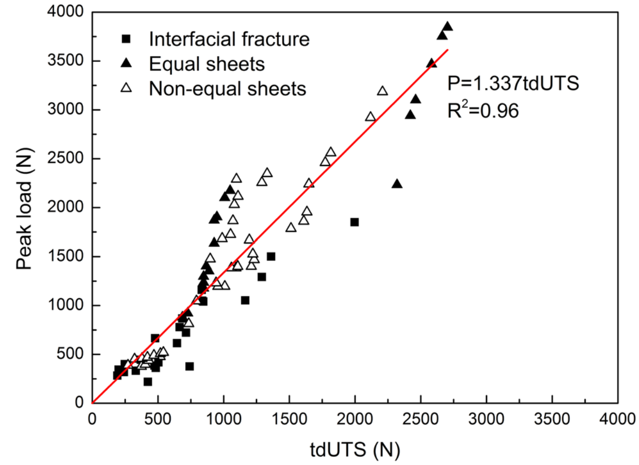

Fig. 15 Peak load vs. (td UTS) for all test data

$$p = C \cdot t \cdot d \cdot (\mathrm{UTS}), \qquad \text{(Eq 1)}$$

where P is the peak load in the tensile test, t is the thickness of the base metal, d is the size of the weld button, UTS is the ultimate tensile strength of the base metal, and C is the proportional constant and is approximately 3.1 for cold-rolled steel and 2.5 for hot-rolled steel. This formula provides a fairly reasonable estimation for a class of steels ranging from low-carbon mild steel to high-strength steels (Ref 18).

Using the sheet thickness t = 2.0 mm for the 2.0/2.0/2.0 combination and t = 1.25 mm for the upper interface and 1.75 mm for the lower interface of the 1.0/1.5/2.0 combination, all data in this study were plotted, as shown in Fig. 15 adopting Eq 1. Figure 15 shows that the linear relation Eq 1 appears to hold both data from the equal and unequal thickness sheets. It also found that the peak loads from welds failed in IF mode tend to be slightly lower than the rest. This is consistent with the previous observations (Ref 22) that the presence of IF in tensile shear tests does not reduce the strength significantly. However, it is cautioned that IF mode fractures in spot welds might have substantially reduced energy absorption capacity as well as strength in normal test such as cross-tension specimen tests.

4.4 Fractographs of the Fracture Surface

The fractographs of the three fracture modes are shown in Fig. 16. In the case of interfacial fracture, an obvious quasi-cleavage fracture was found on the fracture face, as shown in Fig. 16(b) and (c). Both quasi-cleavage fracture (Fig. 16e) and dimples (Fig. 16f) were found in the mixed failure mode. When the weld joint experienced pullout failure, the fracture surface was mainly composed of dimples (Fig. 16h and i). The fractographs confirm that the mechanical properties of weld joint increased gradually from the interfacial failure to pullout failure.

5. Conclusions

Using three-sheet spot welds made of 5052 aluminum alloy, this paper investigates nugget formation during resistance spot welding. Additionally, tensile shear tests were taken to study

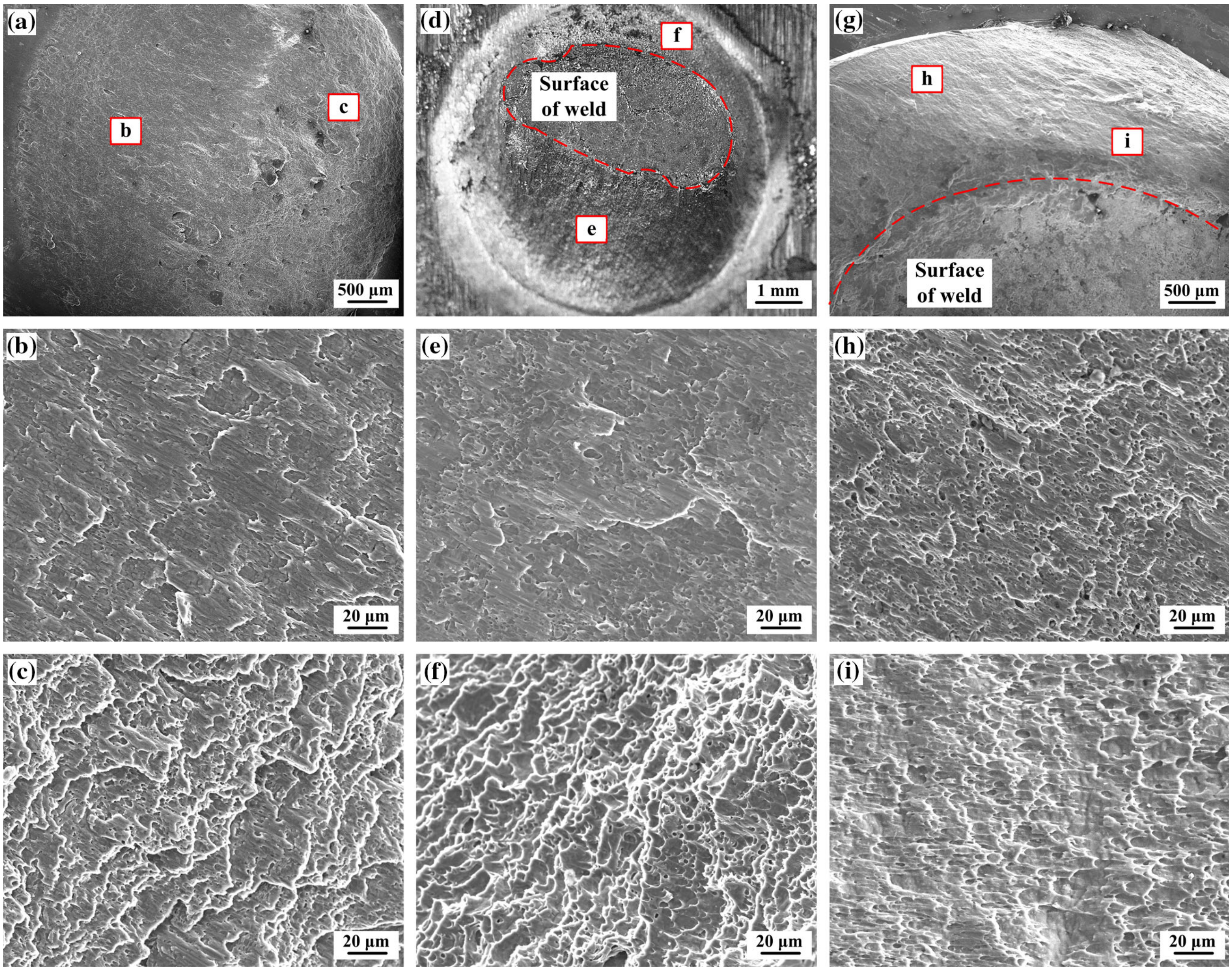

Fig. 16 Micro-morphology of the fracture surfaces: (a)-(c) interfacial failure, (d)-(f) mixed failure, (g)-(i) pullout failure

the mechanical strength and failure mode of the welds. The following conclusions are obtained.

1. For 2.0/2.0/2.0 mm equal thickness sheets, two small nuggets initially formed at the two interfaces. These two nuggets grew slowly along both the radial and axial directions of the workpiece and fused into a big "I"-shaped nugget. With the increase in welding time, the "I"-shaped nugget gradually grew into an elliptical-shaped nugget. The nugget size at the upper interface is slightly bigger than that at the lower interface due to Peltier effect.
2. For 1.0/1.5/2.0 mm unequal thickness sheets, when the welding time was short, two small nuggets initially formed at the two interfaces, and the nugget size at 1.0/1.5 interface was larger than that at the 1.5/2.0 interfaces. As welding time proceeded, the two small nuggets grew along both the radial and axial directions, fused into a big "I"-shaped nugget, and finally became an elliptical nugget. The center of the "I"- or elliptical-shaped nugget gradually shifted toward the geometric center of the three-sheet specimen making the final nugget size at the 1.0/1.5 interface smaller than that at the 1.5/2.0 interface.
3. Similar to the steel spot welds, the failure mode of the current aluminum welds can be one of the three, namely interfacial (IF), mixed or partial pullout (MF), and pullout (PF). The failure mode depends on the welding time or the nugget size at the interface. Short (long) welding time results in smaller (larger) weld nugget and could fail by IF (PF).
4. To interpret the quality of the welds, an average thickness at the interface is proposed for spot welds composed of unequal thickness sheets. All data indicate that the minimum nugget size requirement, $4\sqrt{t}$ (Ref 14), is a good prediction for transition from IF to MF, while the optimum nugget size (Ref 21), $5\sqrt{t}$, ensures the PF mode.
5. The simple formula $P = C{\cdot}t{\cdot}d{\cdot}(UTS)$ appears to hold for both the equal and unequal three-sheet 5052 aluminum alloy spot welds, provided the average thickness at the interface for unequal sheets is used. This formula can be used in transferring the mechanical strength from one weld to another if further verification can be provided.

Acknowledgment

This research is supported by the National Nature Science Foundation of China (Grants 51405334, 51275342, and 51275338) and China Postdoctoral Science Foundation Project (Grant 2013M541175). Y. J. Chao would also like to thank the travel support from China 111 Project (B08040) awarded to the School of Materials Science, Northwestern Polytechnical University, Xian, China.

References

1. J.E. Gould, An Examination of Nugget Development During Spot Welding Using Both Experimental and Analytic Techniques, *Weld. J.*, 1987, **66**(1), p 1-s–10-s
2. W.H. Zhang, X.M. Qiu, D.Q. Sun, and L.J. Han, Effects of Resistance Spot Welding Parameters on Microstructures and Mechanical Properties of Dissimilar Material Joints of Galvanised High Strength Steel and Aluminum Alloy, *Sci. Technol. Weld. Join.*, 2011, **16**(2), p 153–161
3. J.A. Khan, L. Xu, and Y.J. Chao, Prediction of Nugget Development During Resistance Spot Welding Using Coupled Thermal-Electrical-Mechanical Model, *Sci. Technol. Weld. Join.*, 1999, **4**(4), p 201–207
4. A. De and M.P. Theddeus, Finite Element Analysis of Resistance Spot Welding in Aluminium, *Sci. Technol. Weld. Join.*, 2002, **7**(2), p 111–118
5. J. Shen, Y.S. Zhang, X.M. Lai, and P.C. Wang, Modeling of Resistance Spot Welding of Multiple Stacks of Steel Sheets, *Mater. Des.*, 2011, **32**, p 550–560
6. N. Harlin, T.B. Jones, and J.D. Parker, Weld Growth Mechanisms During Resistance Spot Welding of Two and Three Thickness Lap Joints, *Sci. Technol. Weld. Join.*, 2002, **7**(1), p 35–41
7. N. Harlin, T.B. Jones, and J.D. Parker, Weld Growth Mechanism of Resistance Spot Welds in Zinc Coated Steel, *J. Mater. Proc. Technol.*, 2003, **143–144**, p 448–453
8. M. Pouranvari and S.P.H. Marashi, Critical Sheet Thickness for Weld Nugget Growth During Resistance Spot Welding of Three-Steel Sheets, *Sci. Technol. Weld. Join.*, 2011, **16**(2), p 162–165
9. Z.Z. Lei, H.T. Kang, and Y.G. Liu, Finite Element Analysis for Transient Thermal Characteristics of Resistance Spot Welding Process with Three Sheets Assemblies, *Procedia Eng.*, 2011, **16**, p 622–631
10. N. Ma and H. Murakawa, Numerical and Experimental Study on Nugget Formation in Resistance Spot Welding for Three Pieces of High Strength Steel Sheets, *J. Mater. Proc. Technol.*, 2010, **210**, p 2045–2052
11. S. Katayama and Y. Kawahito, Evolution of Laser Welding to Dissimilar Materials Joining, *Trans. JWRI*, 2010, **39**(2), p 268–269
12. V.A. Drebushchak, The Peltier Effect, *J. Therm. Anal. Calorim.*, 2008, **91**(1), p 311–315
13. B. Q. Li, Research on the numerical Simulation of the Process for Aluminum Alloy Resistance Spot Welding and Energy Analysis. Ph.D. Dissertation, 2002, Tianjin, Tianjin University
14. American Welding Society, Test Methods for Evaluating the Resistance Spot Welding Behavior of Automotive Sheet Steel Materials, 2012, AWS D8.9M: 201
15. S. Kou, *Welding Metallurgy*, 2nd ed., Wiley, Hoboken, 2003
16. A. Tavasolizadeh, S.P.H. Marashi, and M. Pouranvari, Mechanical Performance of Three Thickness Resistance Spot Welded Low Carbon Steel, *Mater. Sci. Technol.*, 2011, **27**(1), p 219–224
17. General Administration of Quality Supervision, Inspection and Quarantine of the People's Republic of China. Method of Tensile Test for Welded Joint, 1990, GB 2651-88
18. Y.J. Chao, Ultimate Strength and Failure Mechanism of Resistance Spot Weld Subjected to Tensile, Shear, or Combined Tensile/Shear Loads, *ASME J. Eng. Mater. Technol.*, 2003, **125**(4), p 125–132
19. Y.J. Chao, Failure Mode of Spot Welds: Interfacial Versus Pullout, *Sci. Technol. Weld. Join.*, 2003, **8**(2), p 133–137
20. M. Zhou, H. Zhang, and S.J. Hu, Relationships Between Quality and Attributes of Spot Welds, *Weld. J.*, 2003, **82**(4), p 72-s–77-s
21. R. M. Rivett, Factors Affecting the Quality of Resistance Spot Welds. Ph.D. Dissertation, 1980, Cardiff, Wales, University of Wales
22. J. Sawhill and S. Furr, Spot Weldability Tests for High-Strength Steels, *SAE Paper* 810352, 1981
23. J. Heuschkel, The Expression of Spot-Weld Properties, *Weld. J.*, 1952, **31**(10), p 931-s–943-s